

1. Kitaigorodskii, A. I., in *Order and Disorder in the World of Atoms*, Mir, Moscow, 1980.
2. Mishima, O., Calvert, L. D. and Whalley, E., *Nature*, 1984, **310**, 393–395.
3. Sikka, S. K., in the Proceedings XIII AIRAPT Conference, Bangalore, India, (ed. Singh, A. K.), Oxford and IBH Publishing Co., New Delhi, 1992, p. 254.
4. Peterson, S. W. and Levy, H. A., *Acta Crystallogr.*, 1957, **10**, 70–76.
5. Sosman, R. B., in *The Phases of Silica*, Rutgers University Press, 1965, p. 388.
6. Kuhs, W. F., Finney, J. L., Vettier, C. and Bliss, D. V., *J. Chem. Phys.*, 1984, **81**, 3612–3623.
7. Sinclair, W. and Ringwood, A. E., *Nature*, 1978, **272**, 714–715.
8. Hemley, R. J., Chen, L. C. and Mao, H. K., *Nature*, 1989, **338**, 638–640.
9. Stishov, S. M. and Popova, S. V., *Geochemistry*, 1961, **10**, 923–926.
10. Busing, W. R. and Levy, H. A., *J. Chem. Phys.*, 1957, **26**, 563–568.
11. Meade, C. and Jeanloz, R., *Geophys. Res. Lett.*, 1990, **77**, 1157–1160.
12. Chidambaram, R. and Sikka, S. K. *Chem. Phys. Lett.*, 1968, **2**, 162–165.
13. Steiner, T. H. and Senger, W. S., *Acta Crystallogr.*, 1991, **B47**, 1022–1023.
14. Birch, F., in *Handbook of Physical Constants* (ed. Clark, S. P. Jr.), The Geological Society of America Inc., New York, 1966, p. 97–173.
15. Hazen, R. M., Finger, L. W., Hemley, R. J. and Mao, H. K., *Solid State Commun.*, 1989, **72**, 507–511.
16. Madon, M., Gillet, P., Julien, C. and Price, G. D., *Phys. Chem. Min.*, 1991, **18**, 7–18.
17. Chaplot, S. L. and Sikka, S. K., in the Proceedings XIII AIRAPT Conference, Bangalore, India, (ed. Singh, A. K.), Oxford and IBH Publishing Co., New Delhi, 1992, p. 259.
18. Thathachari, Y. T. and Tiller, W. A., *J. Appl. Phys.*, 1982, **53**, 8615–8619.
19. Ramachandran, G. N. and Sasisekharan, V., *Adv. Protein Chem.*, 1968, **23**, 283–437.
20. Bansal, M. L., in Proceedings of III National Seminar on Ferroelectrics and Dielectrics, India, 1984, p. 77.
21. Sankaran, H., Sikka, S. K., Sharma, S. M. and Chidambaram, R., *Phys. Rev.*, 1988, **B38**, 170–173.

ACKNOWLEDGEMENT. We are grateful to Dr R. Chidambaram for critical and constructive comments.

Received 30 June 1992; accepted 10 July 1992

## Fluid processes in the Earth's lower crust: evidence from microscale isotopic zonation in graphite crystals

M. Santosh\* and H. Wada†

\*Centre for Earth Science Studies, P. B. 7250, Thuruvikkal Post, Trivandrum 695 031, India

†Institute of Geosciences, Faculty of Science, Shizuoka University, Shizuoka 422, Japan

Coarse graphite crystals in a felsic pegmatite dyke at Mannantala, and adjacent to cordierite-rich patches within metapelites at Chittikara in the Kerala Khondalite Belt illustrate crystallization of graphite from CO<sub>2</sub>-rich fluids at temperatures around 700°C. A microscale sampling technique reveals remarkable carbon isotopic zonation within the domain of individual graphite crystals, with lighter cores ( $\delta^{13}\text{C} = -12.5\text{‰}$ ) mantled by heavier rims ( $-10.6\text{‰}$ ). The zonation patterns are correlated with equilibrium isotopic fractionation from CO<sub>2</sub>-rich fluids which infiltrated through structural pathways,

or which were transferred through magmatic conduits. The core compositions of the graphite crystals indicate  $\delta^{13}\text{C}$  values of  $-5$  to  $-6\text{‰}$  for the fluid from which they started crystallizing. This range is identical to the composition of CO<sub>2</sub> trapped within inclusions in the associated minerals, and comparable with CO<sub>2</sub> derived from carbon reservoirs in the subcontinental lithosphere. These results, when coupled with the geodynamics of fluid transfer mechanism in the lower crust, have important bearing on the genesis of gemstone and rare metal mineralization associated with veins and pegmatites.

MAGMATIC, metamorphic and metallogenic processes are often controlled by fluid movements and fluid-rock interaction processes in the earth's deep crust and in the crust-mantle interface. Stable isotopes of carbon, oxygen, hydrogen, nitrogen and sulphur provide important tracers of such fluid processes. Carbon, largely a trace

constituent within the earth, occurs in various forms such as, carbonate minerals, CO<sub>2</sub> trapped as inclusions within minerals, and graphite. Graphite is commonly associated with a variety of supracrustal rocks metamorphosed under a range of pressure-temperature (P-T) conditions, where it is mostly a product of the conversion of organic matter present in ancient sediments<sup>1</sup>. Graphite has also been recorded from ultramafic nodules

\*For correspondence.

and mantle xenoliths, where it occurs as a primary igneous component<sup>2</sup>. The precipitation of graphite from a CO<sub>2</sub>-rich fluid depends largely on the oxygen fugacity conditions of the host rocks at the time of fluid influx. Thermodynamic calculations in the C–O–H system reveal that graphite will precipitate under certain conditions of cooling, fluid mixing, or fluid infiltration into rocks with oxygen buffer capacity<sup>3</sup>. Graphites derived from different settings can be characterized by the relative proportion of the stable isotopes of carbon, namely <sup>13</sup>C and <sup>12</sup>C, expressed by the conventional  $\delta$  notation, and defined as:

$$\delta^{13}\text{C}\text{‰} = \left\{ \left( \frac{{}^{13}\text{C}}{{}^{12}\text{C}} \right)_{\text{graphite}} / \left( \frac{{}^{13}\text{C}}{{}^{12}\text{C}} \right)_{\text{standard}} - 1 \right\} \times 1000,$$

where the standard is a marine carbonate (Chicago Pee Dee Belemnite)<sup>4</sup>. Typical ancient and modern organic carbon has  $\delta^{13}\text{C}$  values lower than  $-25\text{‰}$  (ref. 1). Increasing metamorphic grade may bring about slight variations in this value, but not steep isotopic gradients<sup>5</sup>. On the other hand, graphite precipitated from a CO<sub>2</sub>-rich fluid will have high  $\delta^{13}\text{C}$  values compared to organic carbon. The isotopic fractionation between CO<sub>2</sub> and precipitating graphite is temperature-dependent. For example, equilibrium isotopic fractionation between CO<sub>2</sub> and graphite at 700°C is estimated<sup>6,7</sup> to be around 6–7; this means that the isotopic composition of graphite will be 6–7‰ lighter than that of the CO<sub>2</sub>-rich fluid from which it has crystallized. Experimental studies show that the kinetics of isotopic exchange within graphite are sluggish, so a graphite once fully crystallized is virtually inert, and does not exchange with subsequent fluids, even under high P–T conditions<sup>8,9</sup>. Graphite can hence record important information pertaining to changing fluid regimes.

Until recently, most stable isotopic studies on graphite have relied on conventional bulk sampling techniques<sup>10</sup>. This approach gives only the average isotopic composition of the whole crystal, thereby masking potential information on the fluid behaviour with respect to changing temperature, time and tectonic environment. Recent analytical advances have enabled microsampling of several spots within single crystals<sup>11</sup>. Coupled with high precision stable isotopic measurement<sup>12</sup>, it is now possible to determine carbon isotopic variations within the domain of individual graphite crystals. In this study, we investigate fluid processes in the lower crustal block of the Kerala Khondalite Belt (KKB) of southern India through microscale isotope geochemistry of graphite crystals.

## Geologic background

The Kerala Khondalite Belt is a granulite facies supracrustal sequence forming the southern margin of the

South Indian high grade metamorphic terrain<sup>13</sup>. Evidence for the introduction of CO<sub>2</sub>-rich fluids along structural pathways in this region is provided by the local alteration of amphibolite facies gneisses into desiccated veins and patches of orthopyroxene-bearing granulites ('incipient charnockites')<sup>13,14</sup>. CO<sub>2</sub> influx is also detected from the crystallization of coarse graphite flakes within or adjacent to fluid channels like shears/faults. In this study, we identified two localities where graphite growth resulted from fluids. The first one is at Mannantala quarry, where garnet- and biotite-bearing upper amphibolite facies gneisses show local transformation to incipient charnockites at  $P = 5 \pm 1.9$  kbar,  $T = 725 \pm 25^\circ\text{C}$  and  $X_{\text{H}_2\text{O}} = 0.2 - 0.3$  (ref. 14). A felsic pegmatite dyke adjacent to the arrested charnockite patches (Figure 1) carries coarse graphite flakes (Figure 2). Field relations at Mannantala suggest that the pegmatite dyke was probably the source of CO<sub>2</sub> involved in the gneiss to charnockite dehydration. The second locality is a vertical quarry near the village of Chittikara, exposing garnet-, biotite-, and sillimanite-bearing aluminous metapelites with small grains of cordierite and tiny flakes of organic-derived graphite. The pelitic rocks were metamorphosed at  $P = 4.5 \pm 0.5$  kbar and  $T = 740 \pm 50^\circ\text{C}$  (ref. 15). Veins and patches of coarse graphite

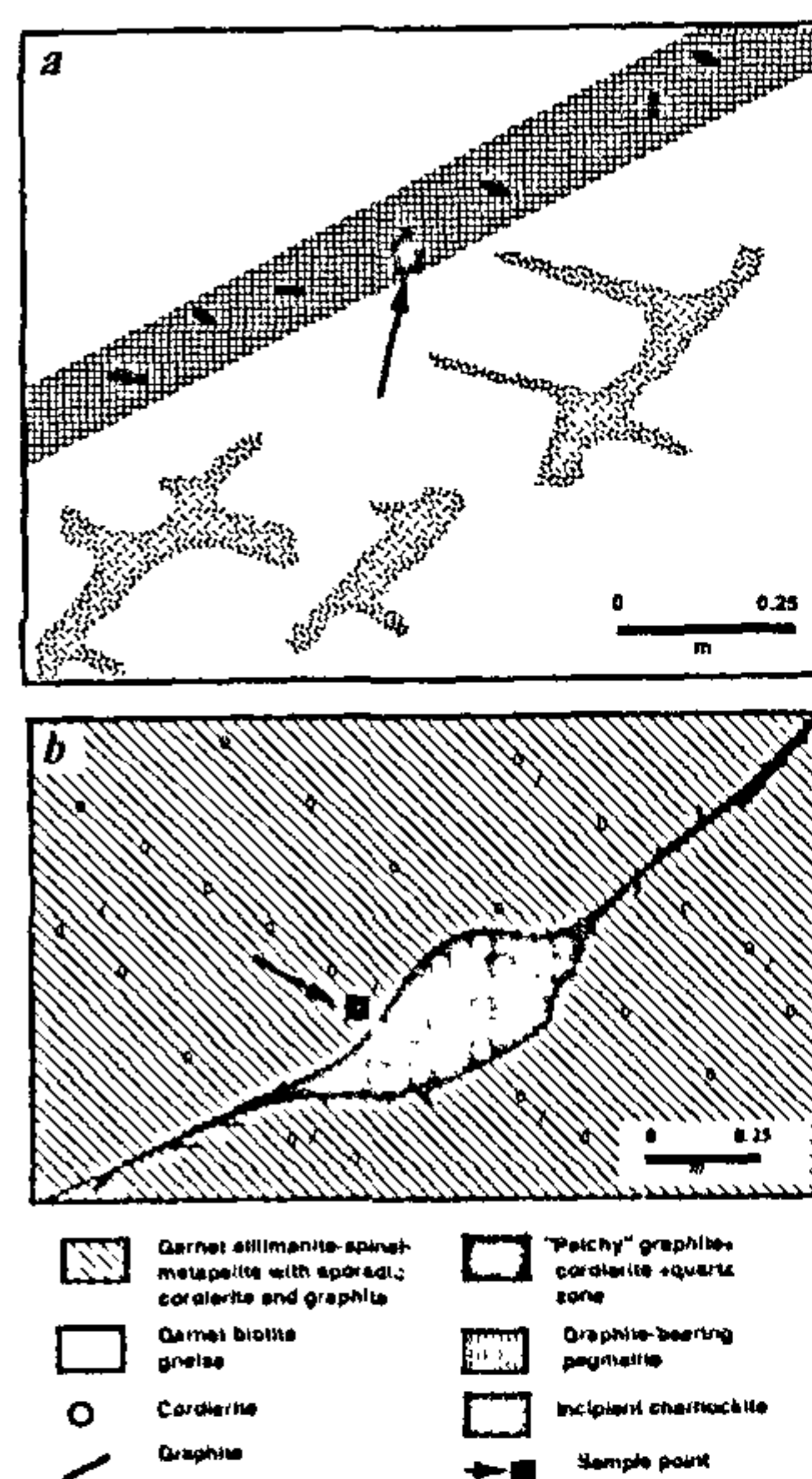


Figure 1. Field relations and sampling points at Mannantala (a) and Chittikara (b) quarries in the Kerala Khondalite Belt



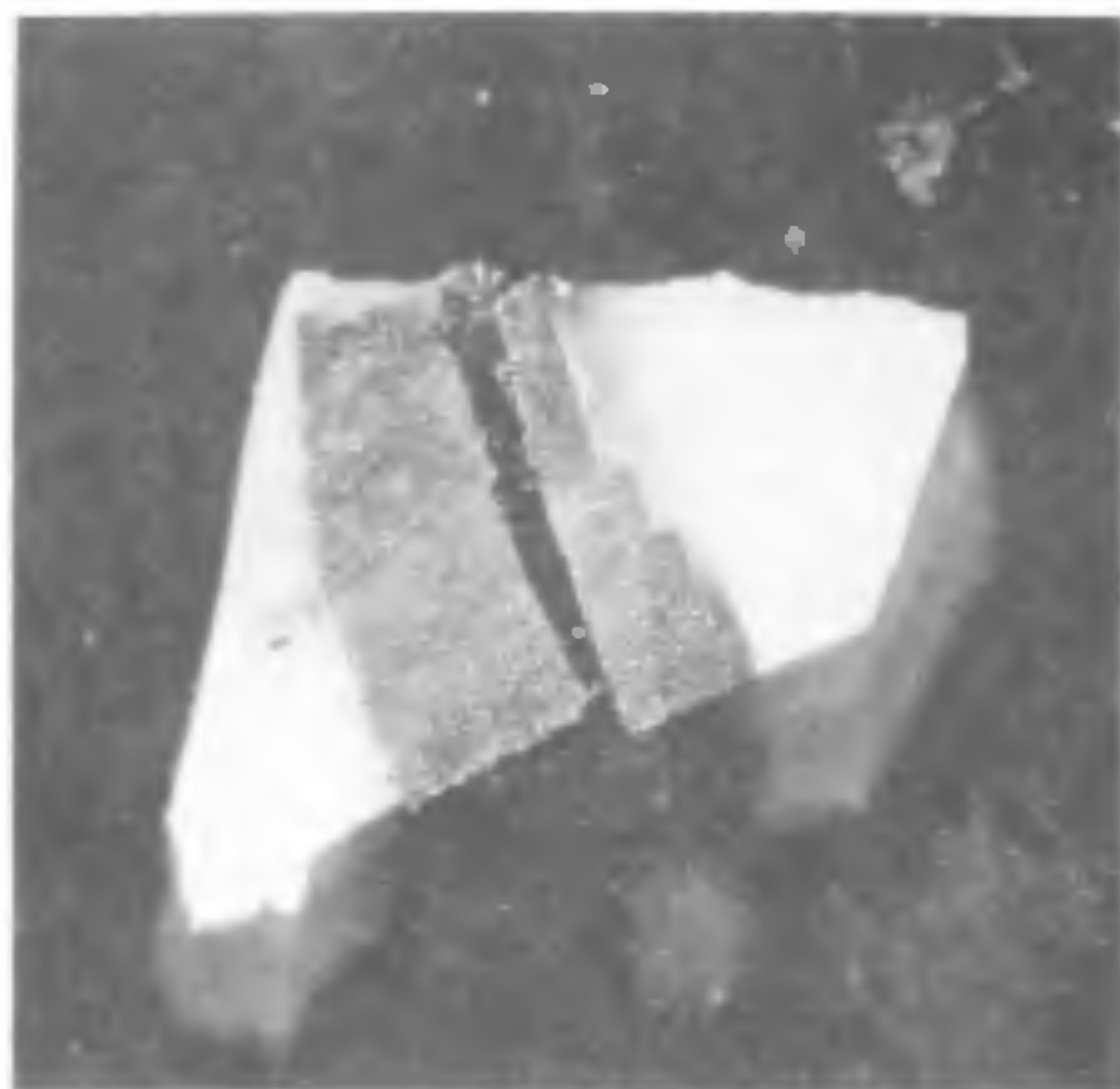


Figure 2. Photomicrograph of graphite crystal from the Mannantala felsic pegmatite, carefully knived at the core for microscale sampling.

along with bluish cordierite and quartz have developed within shears/faults which cross-cut the gneissic fabric (Figure 1). The size of the graphite flakes increases from fraction of a mm in the metapelites to nearly 2 cm adjacent to, and within, the patches and veins. A concomitant increase in abundance of graphite is also noted, from 0.1 volume per cent in the metapelites to nearly 30 volume per cent in the patches and veins. For this study, coarse graphite crystals were collected from the pegmatite at Mannantala, and the host metapelite adjacent to the cordierite-rich patch at Chittikara (cf. Figure 1).

### Microscale isotopic analyses

Graphite crystals were washed with 2N HCl solution. Microsampling involved careful separation of thin films of graphite by keen knife edge, or exfoliation with adhesive tape, perpendicular to the direction of the c-axis of the crystal<sup>11</sup>. Each microsample was scooped up by molybdenum mesh and preheated at 500°C to remove surficial organic contaminants. They were then sealed in Vycor glass tubes, and combusted to CO<sub>2</sub> by reacting with vanadium pentoxide at 1100°C for 2 h. Prior to combustion, the Vycor glass tubes were preheated for over 10 h at 1100°C, and again with sample and vanadium pentoxide at 500°C for 30 min. During our experiments, the blank from Vycor glass tube plus vanadium pentoxide was less than 0.1 µl. The CO<sub>2</sub> evolved from the samples was totally recovered for isotopic analyses. The thickness of each microsample was calculated from the carefully measured area of the flake, and the volume of CO<sub>2</sub> evolved (Table 1). The volume of CO<sub>2</sub> was measured using a specially designed micro-inlet system<sup>9</sup>. Carbon isotopic measurements were performed on a Finnigan MAT-250 mass spectrometer.

### Results

The analytical results are summarized in Table 1, where the isotopic composition of each microsample is reported in the conventional  $\delta$  notation. Microscale isotopic traverses, comprising eight sampling points each from core to margin of graphite crystals from the two localities, were performed. The results show a marked variation in carbon isotopic composition between the core and margin. The Mannantala sample shows  $\delta^{13}\text{C}$

Table 1. Carbon isotopic data from microscale traverses in graphite crystals from Mannantala and Chittikara

Sample	Distance from grain margin (µm)	Area (mm <sup>2</sup> )	Thickness (µm)	Volume of CO <sub>2</sub> (µl)	$\delta^{13}\text{C}$ (‰)
Mannantala	6	0.47	13.0	24.93	-10.88
	19	0.15	15.0	9.50	-10.89
	34	0.31	7.5	9.64	-11.09
	41	0.39	18.0	29.69	-11.08
	59	0.44	53.0	97.82	-10.83
	500	0.47	18.0	34.52	-11.03
	800	0.88	156.0	57.45	-10.60
	1000	0.56	33.0	77.07	-12.08
Chittikara	35	0.36	71.0	107.22	-11.09
	80	0.75	21.0	66.86	-11.58
	105	0.60	31.0	78.50	-11.40
	420	0.25	100.0	121.00	-12.30
	535	0.28	130.0	132.00	-12.35
	788	0.15	75.0	112.50	-12.44
	895	0.75	140.0	170.40	-12.52
	995	0.75	56.0	175.99	-12.02

value of  $-12.1\text{‰}$  for the core, and  $-10.6\text{‰}$  for the margin. The core composition of the Chittikara graphite is identical to this value, at  $-12.5\text{‰}$ . Its rim composition ( $-11.1\text{‰}$ ) is slightly lower than the Mannantala sample. Importantly, in both cases, the cores of the crystals are characterized by lighter carbon, and the rims show enrichment in  $^{13}\text{C}$ .

The core to rim variations in  $\delta^{13}\text{C}$  in the two samples are plotted in Figure 3. In the Mannantala graphite, an abrupt change from lighter to heavier carbon enrichment adjacent to the core is observed, within a distance of  $200\text{ }\mu\text{m}$  towards the margin. After this 'step-function', the  $\delta^{13}\text{C}$  values are broadly constant ( $11 \pm 0.5\text{‰}$ ) in the remaining part of the crystal. On the other hand, the Chittikara sample shows a progressive enrichment in  $^{13}\text{C}$  from the core towards the margin.

## Discussion

The range of carbon isotopic values obtained in this study ( $-10.6$  to  $-12.5\text{‰}$ ) is high and markedly different from the  $\delta^{13}\text{C}$  values of graphites derived by the metamorphism of organic carbon ( $< -25\text{‰}$ )<sup>1</sup>. Indeed, disseminated graphite in the host gneisses in these localities has low  $\delta^{13}\text{C}$  values; at Chittikara they show  $-34\text{‰}$  (ref. 14). Our results hence indicate that the coarse graphite flakes within the pegmatite at Mannantala and adjacent to the cordierite-rich patches at Chittikara were precipitated from  $\text{CO}_2$ -rich fluids. Temperature estimates from mineral phase equilibria lie around  $700^\circ\text{C}$  in both localities<sup>14,15</sup>. Equilibrium fractionation between  $\text{CO}_2$  and graphite at this temperature<sup>6,7</sup> suggests that the parental fluid from which the graphite cores started crystallizing had a  $\delta^{13}\text{C}$  composition of  $-5$  to  $-6\text{‰}$ .

The most important aspect revealed in this study is

the existence of marked isotopic zonations in the scale of micrometers within individual graphite crystals, which is a direct reflection of the temperature- and time-integrated geochemical evolution of the fluids from which the graphites crystallized. A direct, bulk precipitation of graphite from the  $\text{CO}_2$ -rich fluid would only have produced isotopically homogeneous, unzoned crystals. On the other hand, the Chittikara graphite displays progressive rimward increase in  $\delta^{13}\text{C}$ , whilst at Mannantala, an initial rimward enrichment in  $^{13}\text{C}$  is followed by near-constant isotopic composition in the remaining part of the crystal. These contrasting stable isotopic profiles among localities within the same deep crustal segment suggest that local kinetic factors exert significant influence on fluid movements in the lower crust.

Precipitation of graphite from a  $\text{CO}_2$ -rich fluid can be modelled by the two endmember situations of isotopic fractionation namely, Rayleigh fractionation, and batch fractionation<sup>10,16</sup>. Under Rayleigh fractionation, the rate of crystal growth far exceeds the time-scales required to maintain isotopic equilibrium; consequently the high precipitation rate coupled with the slow exchange rate in graphite would produce isotopically zoned crystals. The progressive rimward increase of  $\delta^{13}\text{C}$  in graphite from Chittikara indicates that incremental precipitation of graphite occurred through a Rayleigh-type fractionation process, where the initial composition of the fluid became progressively enriched in  $^{13}\text{C}$ , concomitant with the crystallization of the outer zones of the crystal (Figure 4). The zone of coarse cordierite + graphite represents a fluid channel, where the graphites show extreme zonation and the cordierites preserve multiple entrapment of fluids<sup>15</sup>. Advection of  $\text{CO}_2$  across this fluid channel up to a few cm into the host metapelites resulted in graphite precipitation adjacent to the patchy zone. The rim composition of the Chittikara graphite represents the stage at which fluid

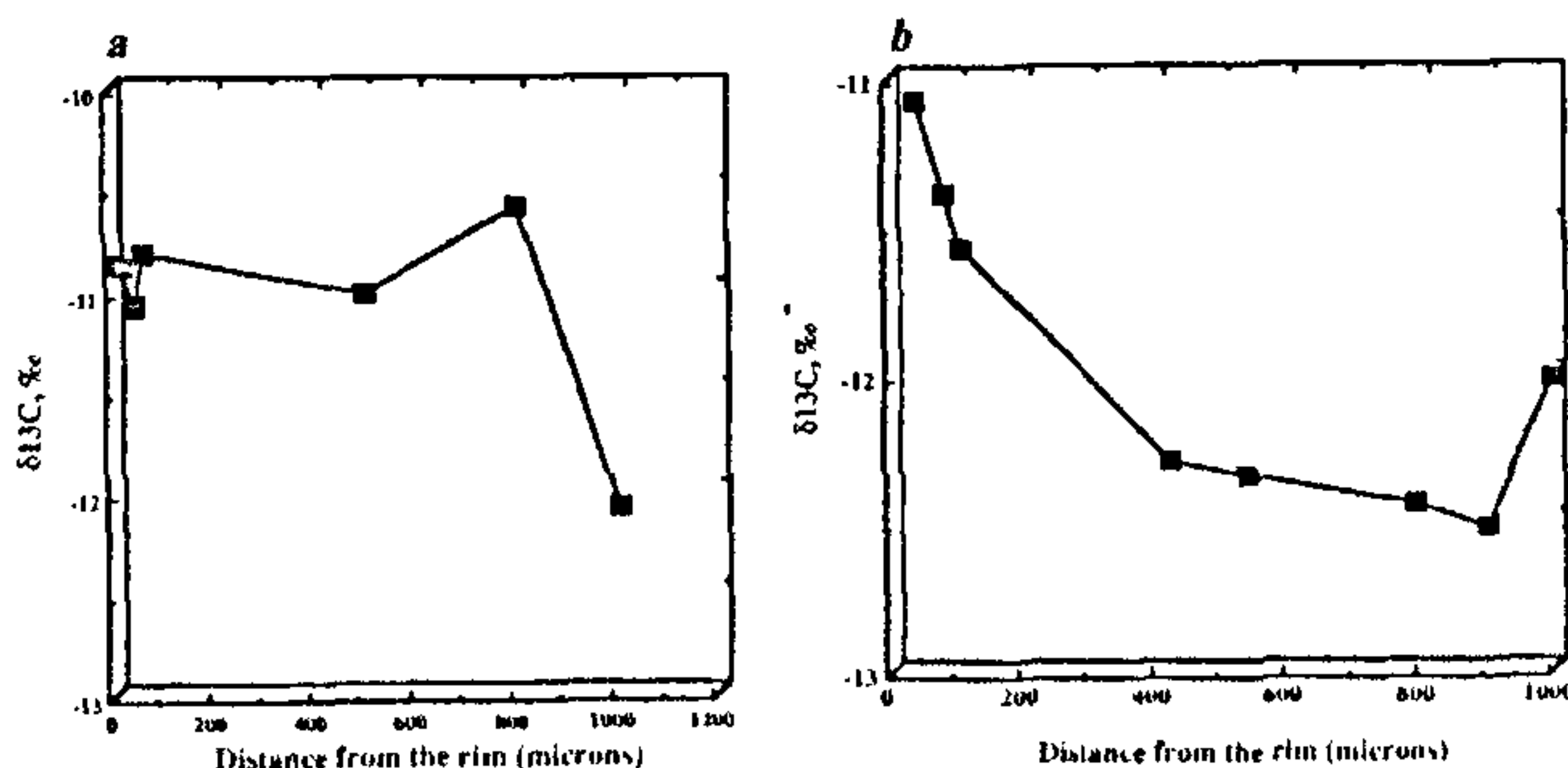


Figure 3. Microscale carbon isotopic variation in graphite crystal from Mannantala (a) and Chittikara (b)



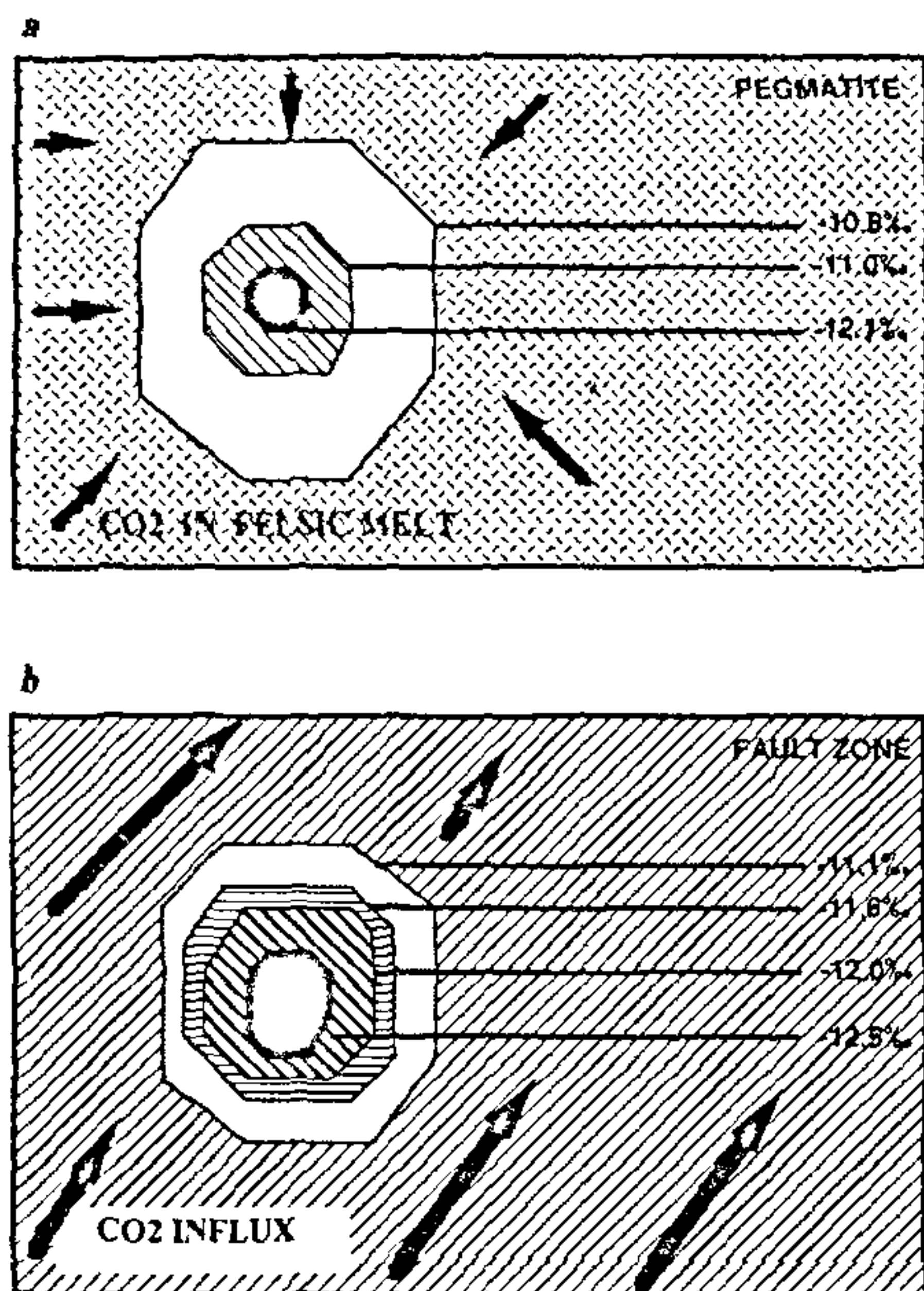


Figure 4. Schematic diagram showing the isotopic zonation patterns in graphite crystals from Mannantala (a) and Chittikara (b). These patterns are correlatable with distinct modes of equilibrium isotopic fractionation from  $\text{CO}_2$ -rich fluids outgassed from a carbon reservoir in the subcontinental lithosphere. See text for details.

advection culminated, and all the fluids were consumed.

The microscale isotope geochemistry of Mannantala graphite probably represents a two-stage process involving an initial Rayleigh-type fractionation, followed by batch fractionation. Here, it is envisaged that a  $\text{CO}_2$ -enriched pegmatite melt was emplaced into the reduced country rocks, where disseminated organic graphite acted as an effective oxygen buffer. This triggered two processes: 1) precipitation of graphite from the melt in response to change in  $f\text{O}_2$ , and 2) degassing of the melt and release of  $\text{CO}_2$  due to change in  $P$ - $T$ . The  $\text{CO}_2$  released from the felsic melt could have been the vector for local dehydration and desiccation of the gneisses into veins and patches of incipient charnockites. Where the rate of crystallization of graphite exceeds the rate of introduction of fluids, isotopic fractionation is of batch-type, allowing sufficient time-scales to attain isotopic equilibrium with the fluid. Crystallization of the felsic melt represents slow cooling in a closed system, where there is no external introduction of fluids. Such a process would be incapable of producing isotopic zonation, as

illustrated by the near-constant  $\delta^{13}\text{C}$  values for the subsequent rimward zones in the Mannantala graphite.

Our study has important bearing on the geodynamics of fluid transfer in the lower crust. The  $\delta^{13}\text{C}$  values recorded by the graphite crystals indicate carbon isotopic composition of  $-5$  to  $-6\%$  for the fluids from which they started crystallizing, under equilibrium isotopic fractionation. These values are identical with the ranges recorded from  $\text{CO}_2$  trapped within inclusions in the associated minerals<sup>14,15</sup>. Carbon isotopic compositions of diamonds, carbonatites,  $\text{CO}_2$  trapped within Mid Ocean Ridge Basalts, and such other potential settings of mantle-derived carbon also display similar ranges<sup>17</sup>. This suggests that  $\text{CO}_2$ -rich fluids which infiltrated this lower crustal segment were derived from a homogeneous carbon reservoir in the subcontinental lithosphere. The fluids were transferred to lower and middle crust through magmatic conduits or structural pathways. Mantle-derived  $\text{CO}_2$ - $\text{H}_2\text{O}$  fluids are potential carriers of precious metals, rare earths and rare metals, which they scavenge during their migration to higher crustal levels. Occurrences of a wide variety of mineralized pegmatite belts have been recorded from the KKB<sup>18</sup>. These include gemstone-bearing categories, especially with prized chrysoberyls, and rare metal pegmatites carrying columbite and tantalite.  $\text{CO}_2$ -rich fluid inclusions and coarse graphite flakes are often associated with these occurrences. The coarse, gemmy cordierite at Chittikara, and monazite crystals in pegmatites at Mannantala also derive attention in this regard. It is suggested that intensified exploration in localities which bear imprints for the transfer of  $\text{CO}_2$ -rich fluids from deep reservoirs may prove worthwhile in identifying potential mineralization.

1. Eichmann, R. and Schidlowski, M., *Geochim. Cosmochim. Acta*, 1975, **39**, 589-595
2. Pineau, F., Javoy, M. and Kornprobst, J., *J. Petrol.*, 1987, **28**, 313-322.
3. Lamb, W. M. and Valley, J. W., *Nature*, 1984, **312**, 56-58.
4. Craig, H., *Geochim. Cosmochim. Acta*, 1953, **3**, 53-92.
5. Dunn, S. R. and Valley, J. W., *J. Metamorphic Geol.*, 1992, (in Press).
6. Wada, H. and Suzuki, K., *Geochim. Cosmochim. Acta*, 1983, **47**, 697-706.
7. Chacko, T., Kumar, G. R. R. and Newton, R. C., *J. Geol.*, 1987, **95**, 343-358.
8. Valley, J. W. and O'Neil, J. R., *Geochim. Cosmochim. Acta*, 1981, **45**, 411-419.
9. Wada, H., Ando, T., Iwaki, K. and Arita, Y., 7th ICOG Canberra, 1990 (abstr.).
10. Farquhar, J. and Chacko, T., *Nature*, 1991, **354**, 60-63.
11. Wada, H., *Nature*, 1988, **331**, 61-63.
12. Wada, H. and Ito, R., *Mass Spectrometry*, 1990, **38**, 287-294.
13. Chacko, T., Mayeda, T. K., Clayton, R. N. and Goldsmith, J. R., *Geochim. Cosmochim. Acta*, 1991, **55**, 2867-2882.
14. Santosh, M., Harris, N. B. W., Jackson, D. H. and Matthey, D. P., *J. Geol.*, 1990, **98**, 915-926.
15. Santosh, M., Jackson, D. H. and Harris, N. B. W., *J. Petrol.*, 1992, (in press).



16. Valley, J. W., in *Reviews in Mineralogy*, (eds. Valley, J. W., Taylor, H. P. and O'Neil, J. R.), 1986, vol. 16, pp. 445-481.
17. Javoy, M., Pineau, F. and Delorme, H., *Chem. Geol.*, 1986, **57**, 41-62.
18. Soman, K., Unpublished PhD thesis, People's Friendship University, Moscow, 1980.

ACKNOWLEDGEMENTS. M. S. thanks the Department of Science and Technology, Government of India, for project support to study deep crustal fluid processes.

Received 21 July 1992; accepted 27 July 1992

## Thermally induced structural changes in wool: A high-resolution solid-state carbon-13 CPMAS NMR study

N. R. Jagannathan\*, Ashok A. Itagi<sup>†</sup> and V. Subramaniam<sup>†</sup>

\*Department of Crystallography and Biophysics, University of Madras, Guindy Campus, Madras 600 025, India

<sup>†</sup>Department of Textile Technology, A. C. College of Technology, Anna University, Madras 600 025, India

Carbon-13 CPMAS NMR spectra of merino fine wool fibre (Quality 64S) were recorded as a function of heating from room temperature to 190°C. At about 170°C, the unsaturation of aromaticity increases. Analysis of the observed chemical shift values (at 170°C) of the main chain carbonyl carbons reveal that both the right-handed  $\alpha$ -helix and  $\beta$ -sheet forms exist in the wool fibre.

SOLID-STATE NMR is a powerful and versatile tool for the study of structure, morphology and dynamics of biopolymeric systems. It is well documented in the literature that the carbon-13 chemical shifts of biological molecules in the solid state observed through the cross-polarization and magic angle spinning (CPMAS) techniques are conformation dependent<sup>1</sup>. In particular, the C-13 chemical shifts in polypeptides and other systems arise mainly from the local conformation of the amino-acid residues and are not strongly influenced by the specific amino-acid sequences. The chemical shifts are therefore interpretable in terms of secondary structural features such as  $\alpha$ -helix,  $\beta$ -sheet,  $\omega$ -helix and  $3_1$ -helix<sup>1</sup>.

C-13 CPMAS NMR studies of silk<sup>2-5</sup>, collagen<sup>6</sup>, elastin<sup>7</sup> and tropomyosin<sup>8</sup> have demonstrated that this technique is very useful for obtaining information about the secondary structure of these molecules. On the other hand, studies relating to wool are meagre<sup>1,9</sup> and we report here the results of a study of the conformational response to thermal heating of the merino fine wool (Quality 64S).

In spite of its long use as a fibre, the structure and

morphology of wool is still not understood well. Wool is relatively more complex in composition and structure than silk and it contains a large number of amino acid side chains of all types occurring in different proportions<sup>10</sup>. On the basis of X-ray diffraction data, native wool can be divided into two general categories: the  $\alpha$ - and  $\beta$ -keratins. Chemical analyses indicate that no particular amino acid predominates but that there is a high content of polar residues, cysteine and proline in the keratins. It is in fact surprising that the keratins give such 'crystalline' X-ray fibre patterns even in the presence of these polar residues. However, the heavy cross-linking, presumably derived from S-S bridges, renders keratins in the native state difficult to characterize. The non-crystalline material acts as a highly cross-linked amorphous polymer in a rubbery state<sup>10,11</sup>.

Much of the complexity of wool behaviour and the effects of temperature, stress and chemical reagents are due to two factors: (a) the ease of occurrence of the crystal transitions from  $\alpha$  to  $\beta$  or to random coil, and (b) the ease of breakdown of cross links in amorphous regions and the formation of new ones. Moreover, X-ray diffraction study also indicates that if the heating is sufficiently small, the phase change at the molecular level is from the  $\alpha$ -helical structure to the  $\beta$ -extended structure. On the other hand, if the rate of heating is sufficiently high and cooling is rapid little or no  $\beta$ -structure is formed. In fact, there may be recrystallization of  $\alpha$  material. Therefore, at a low heating rate the change that takes place is  $\alpha \rightarrow \text{noncrystalline} \rightarrow \beta$  with a small entropy and heat change. If the heating rate is sufficiently high it is from  $\alpha \rightarrow \text{noncrystalline}$  with large entropy and heat change<sup>12</sup>. The complexity of wool keratin structure and its behaviour with heating, prompted us to study the material by solid state C-13 CPMAS NMR with a view to understand the effects of heat on wool fibres and to arrive at some conclusion regarding the unsaturation of wool and the conformational changes.

Merino fine wool fibres (Quality 64S) were cleaned by subjecting them to petroleum ether extraction. The cleaned fibres were dried at room temperature and samples of about 1 g were heat-treated in an oven under atmospheric conditions at 120°, 150°, 170° and

\*For correspondence